Promoting Role of $[PtI_2(CO)]_2$ in the Iridium-Catalyzed Methanol Carbonylation to Acetic Acid and Its Interaction with Involved Iridium Species

Samuel Gautron,[†,‡] Nicolas Lassauque,[†] Carole Le Berre,[†] Laurent Azam,[†] Roberto Giordano,[†] Philippe Serp,[†] Gábor Laurenczy,[§] Jean Claude Daran,[||] Carine Duhayon,[||] Daniel Thiébaut,[‡] and Philippe Kalck*[,†]

Laboratoire de Catalyse, Chimie Fine et Polymères, Ecole Nationale Supérieure d'Ingénieurs en Arts Chimiques Et Technologiques (ENSIACET), 118 route de Narbonne, F-31077 Toulouse Cedex 4, France, ACETEX CHIMIE, Acetic Acid Task Force One, AATF1, Usine de Pardies, BP 17, 64150 Mourenx, France, Institut des Sciences et Ingénierie Chimiques, BCH-LCOM, Ecole Polytechnique Fédérale de Lausanne, CH-1015 Lausanne, Switzerland, and Laboratoire de Chimie de Coordination du CNRS, 205 route de Narbonne, 31077 Toulouse Cedex, France

Received March 30, 2006

The catalytic activity of the iridium complexes involved in methanol carbonylation is significantly enhanced when the carbonyliodoplatinum dimer $[PtI_2(CO)]_2$ (**10′**) is added to the reaction mixture. Under CO this complex readily affords the monomeric species $[PtI_2(CO)_2]$ (**10**). The turnover frequency value, which is 1450 h^{-1} for iridium alone, reaches 2400 h^{-1} for a Pt/Ir = 3/7 molar ratio, under 30 bar of CO and at 190 °C. To get a deeper insight into the role of the platinum cocatalyst, model conditions (dinitrogen, ambient temperature, CH_2Cl_2, PPN^+ as counterion) have been adopted. $[PtI_2(CO)]_2$ (**10′**) interacts with $[PPN][IrI_3(CH_3)(CO)_2]$ (**4-PPN**), affording the monoiodo-bridged anionic species $[IrI_2(CH_3)(CO)_2(\mu\text{-}I)\text{-}PtI_2(CO)]^-$ (**11**), which undergoes cleavage under CO to provide $[IrI_2(CH_3)(CO)_3]$ (**6**) and $[PtI_3(CO)]^-$ (**9**). Although we have to take into account the possible iodide dissociation from **4** in the polar reaction medium (CH_3COOH, CH_3OH, CH_3I, HI, H_2O), which can be scavenged by platinum to give **9**, we should not discard the intermediacy of **11**, even under working catalytic conditions. The crystal structures of $[PPN][IrI_3(COCH_3)(CO)_2]$ (**8-PPN**) and $[PPN][PtI_3(CO)]$ (**9-PPN**), which are both involved in the overall process, were determined by X-ray diffraction analysis. A catalytic cycle is herein proposed, in which the cooperative effect between the platinum promoter and the iridium catalyst is depicted.

Introduction

To ensure the annual worldwide production of more than 8 million tons of acetic acid, methods other than carbonylation of methanol are economically obsolete.[1] Among the group VIII metals that have been recognized as catalysts for this reaction, cobalt diiodide, which was the first catalytic precursor to be discovered and then used in a small plant in the 1960s, requires harsh conditions of 680 bar of CO and 250 °C and is now only of historical interest.[2,3] In 1970, Monsanto developed a new low-pressure process, based on both rhodium and an iodide promoter, characterized by very mild conditions (30 bar, 190 °C).[4] Oxidative addition of CH_3I to the $H[RhI_2(CO)_2]$ active species was shown to be the rate-determining step.[5] The main concern in this process is the high energy costs to separate water from acetic acid by distillation;[3] indeed, below a 14 wt % water concentration, precipitation of a rhodium iodide salt occurs. At low water concentrations, Celanese has shown that the introduction of large amounts of LiI significantly stabilizes the rhodium catalyst.[6]

Iridium is also capable of catalyzing methanol carbonylation, but, although it tolerates low water concentrations and low CO pressures, its activity is too low in comparison to that of rhodium to anticipate any industrial application.[7] BP Chemicals discovered that the addition of a ruthenium promoter enabled a viable mixed catalytic system.[8] Addition of such a compound increases both the stability and the catalytic activity.[9,10a] Experiments conducted on the Ir−Ru system showed that the main role of $[RuI_2(CO)_4]$ is to act as an iodide abstractor, facilitating conversion of $[IrI_3(CH_3)(CO)_2]^-$ (**4**) into the key species $[IrI_2(CH_3)(CO)_3]$ (**6**), which in turn rapidly undergoes CO insertion with

* To whom correspondence should be addressed. E-mail: Philippe.Kalck@ensiacet.fr.

† Ecole Nationale Supérieure d'Ingénieurs en Arts Chimiques Et Technologiques (ENSIACET).

‡ ACETEX CHIMIE.

§ Ecole Polytechnique Fédérale de Lausanne.

|| Laboratoire de Chimie de Coordination du CNRS.

(1) Weissermel, K.; Arpe, H. J. In *Industrial Organic Chemistry*, 3rd ed.; VCH: Weinheim, Germany, 1997.

(2) Torrence, P. In *Applied Homogeneous Catalysis with Organometallic Conpounds*; Cornils B., Herrmann W. A., Eds.; Wiley-VCH: Weinheim, Germany, 2002; p 104.

(3) Noriyuki, Y.; Kusano, S.; Yasui, M.; Pujado, P. W. *Appl. Catal.* **2001**, *221*, 253.

(4) Paulik, F. E.; Hersman, A.; Knox, W. R.; Roth, J. F. (Monsanto Co.) U.S. Patent 3,769,329, 1973.

(5) Forster, D. *Adv. Organomet. Chem.* **1979**, *17*, 225.

(6) Smith, B. L.; Torrence, G. P.; Aguilo, A.; Alder, S. (Hoechst Celanese Corp.) U.S. Patent 5,001,259, 1991.

(7) Jones, J. H. *Platinum Met. Rev.* **2000**, *44*, 94.

(8) Vercauteren, C. J. E.; Clode, K. E.; Watson, D. J. Eur. Patent 616,-997, 1994.

(9) Whyman, R.; Wright, A. P.; Iggo, J. A.; Heaton, B. T. *Dalton Trans.* **2002**, 771.

(10) (a) Haynes, A.; Maitlis, P. M.; Morris, G. E.; Sunley, G. J.; Adams, H.; Badger, P. W.; Bowers, C. M.; Cook, D. B.; Elliott, P. I. P.; Ghaffar, T.; Green, H.; Griffin, T. R.; Payne, M.; Pearson, J. M.; Taylor, M. J.; Vickers, P. W.; Watt, R. J. *J. Am. Chem. Soc.* **2004**, *126*, 2847. (b) Maitlis, P. M.; Haynes, H.; Sunley, G. J.; Howard, M. J. *J. Chem. Soc., Dalton Trans.* **1996**, 2187.

10.1021/om060282x CCC: $33.50
Publication on Web 11/08/2006

formation of the acyl complex **8**.[10a,b] The Ru promoter can also act as a scavenger of free HI released during catalysis.

During our studies of the promoting effect of the platinum dimer $[PtI_2(CO)]_2$ on the iridium-catalyzed methanol carbonylation at low water concentrations,[11a,b] which showed catalytic efficiency close to that of ruthenium, we gained spectroscopic and FAB-MS evidence of the formation of a heterobimetallic monoiodo-bridged [Ir−Pt] species having structural features similar to those detected and characterized by Whyman et al.[9]

Results and Discussion

In most literature reports, the catalytically active iridium species is considered to be $H[IrI_2(CO)_2]$ (**1-H**).[12] We have directly generated it in situ by heating in an autoclave an acetic acid/water solution containing a suspension of an iridium iodide salt (a mixture of IrI_3 and IrI_4), under 6 bar of CO at 190 °C for 25 min. After this preformation treatment, the carbonylation of methanol/methyl iodide mixtures to acetic acid was performed under 30 bar of CO under the very conditions used in the industrial Monsanto process, except for a 6 wt % water concentration. This iridium system gives only modest carbonylation rates, since the maximum turnover frequency observed is 1450 h^{-1}. Under the same catalytic conditions, the addition of the dimer $[PtI_2(CO)]_2$ (**10′**) significantly enhances the catalytic activity. The TOFs calculated exclusively on the basis of the iridium concentrations in the medium reach 2400 h^{-1}. The highest activity was obtained for a Pt/Ir molar ratio of 3/7 and a water concentration between 5 and 6 wt %.[11a] These results approach those obtained with the iridium−ruthenium system used in the Cativa process, which is now being implemented in industrial plants.[7]

By separate experiments we have demonstrated that the carbonyliodoplatinum dimer alone presents no catalytic activity: in the same way as ruthenium, it plays the role of cocatalyst.

1. Mechanistic Studies of the Preformation of Iridium Active Species. It is largely admitted in the literature[13] that two anionic catalytic cycles are interconnected for iridium (Scheme 1), one for the carbonylation of methanol and the other for the WGSR (water-gas shift reaction), which constitutes an undesirable side process. These two cycles are linked by the active species $H[IrI_2(CO)_2]$ (**1-H**). We have followed by high-pressure IR (CIR) and high-pressure NMR the in situ preformation of complex **1-H**. The commercial salt IrI_3/IrI_4 was reacted in a 20/1 chlorobenzene/water mixture (w/w) at 130 °C and under 5 bar of CO. Infrared spectra show the progressive appearance of four bands at 2163 w, 2112 vs, 2064 vs, and 1982 m cm^{-1}, which we can assign to the presence of both $H[Ir(H)I_3(CO)_2]$ (**2-H**: ν_{IrH} 2163 cm^{-1}; ν_{CO} 2112, 2064 cm^{-1}) and **1-H** (ν_{CO} 2064, 1982 cm^{-1}) by comparison with the spectra of [PPN]-$[Ir(H)I_3(CO)_2]$ (**2-PPN**) and $[PPN][IrI_2(CO)_2]$ (**1-PPN**), respectively, which were also fully characterized by X-ray diffractometry.[14]

The ν_{IrH} and ν_{CO} bands of **2-PPN** and **1-PPN** slightly differ from those observed for **2-H** and **1-H**, respectively (Table 1).

Scheme 1. Catalytic Cycle for the Iridium-Catalyzed Methanol Carbonylation to Acetic Acid

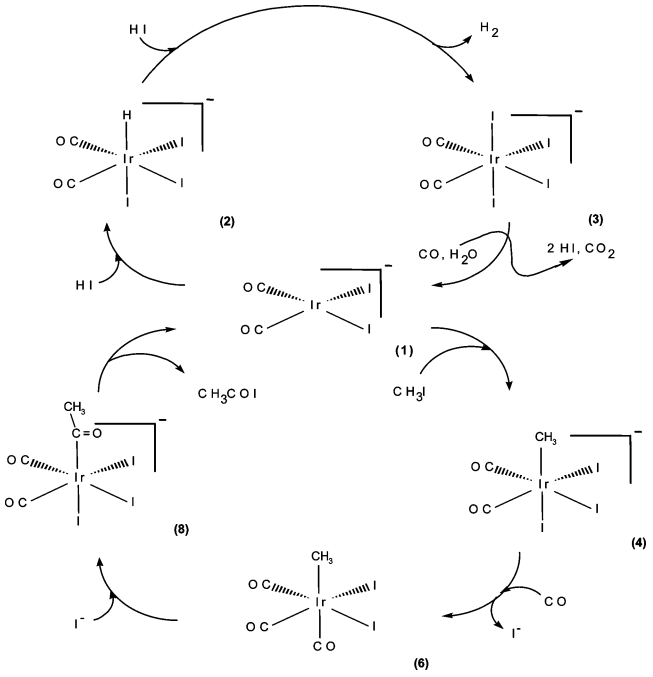

We have also monitored the formation of the hydride complex by HP-NMR under the same preformation conditions, at 90 °C. In the ^1H NMR spectrum (Figure 1), a hydride signal is observed at δ_H −11.6 ppm, very close to the −11.7 ppm value already reported for **2-PPN**, thus confirming the presence of **2-H** in the medium.[14]

We performed other series of experiments under conditions as close as possible to those of catalysis, so as to obtain valuable information about the long-lived complexes involved in the catalytic cycle. For this purpose we avoided the use of stabilizing counterions, such as PPN^+ and $AsPh_4^+$, and/or the use of deuterated organic solvents. Indeed, HP-NMR experiments were performed in acetic acid/water (90/10) solutions under 30 bar of CO and at 90 °C, with the IrI_3/IrI_4 salt. This salt reacts within 30 min to provide almost exclusively **2-H** (characterized by δ_H −11.5 ppm and δ_C 156.0 ppm). In addition, two weak ^{13}C NMR signals were detected at 163.4 and 151.3 ppm (Figure 2) and assigned to the presence of *cis*- and *trans*-$[H][IrI_4(CO)_2]$ (**3-H**). We also observed an intense signal at 125.0 ppm, due to the presence of significant amounts of dissolved CO_2, which points to the fact that iridium catalyzes the WGSR in the absence of iodomethane. Moreover, and unexpectedly, complex **1-H** is not observed as the resting state in the preformation process. Presumably, as the medium contains some amounts of HI, released through the reduction of IrI_3/IrI_4 by CO, the oxidative addition of HI to **1-H** occurs so quickly that **2-H** becomes the resting state in the WGSR.

2. Behavior of 1-PPN and 1-H under Carbonylation Conditions. 2.1. Schlenk Experiments on 1-PPN Reactivity. We have reported previously[14] that **1-PPN** reacts preferentially with HI to give **2-PPN**, even in the presence of a 40-fold excess of CH_3I, so that the shift from WGSR to methanol carbonylation occurs only at a slow rate. The oxidative addition of CH_3I to **1** proceeds reversibly at elevated temperature,[12] producing the anionic methyliridium species **4**. In a previous study we had isolated the complex **4-PPN**, the X-ray crystal structure of which is consistent with that of a fac,cis isomer.[14] The rate-determining

(11) (a) Le Berre, C.; Serp, P.; Kalck, P.; Layeillon, L.; Thiebaut, D. (Acetex Chimie) Fr. Patent 9,813,954, 1998. (b) Gautron, S.; Lassauque, N.; Le Berre, C.; Serp, P.; Azam, L.; Giordano, R.; Laurenczy, G.; Thiébaut, D.; Kalck P. *Eur. J. Inorg. Chem.* **2006**, *6*, 1121.

(12) (a) Forster, D. *J. Chem. Soc., Dalton Trans.* **1979**, 1639. (b) Vickers, P. W.; Pearson, J. M.; Ghaffar, T.; Adams, H.; Haynes, A. J. *J. Phys. Org. Chem.* **2004**, 17, 1007.

(13) Forster, D.; Singleton, T. C. *J. Mol. Catal.* **1982**, 299.

(14) Gautron, S.; Giordano, R.; Le Berre, C.; Jaud, J.; Daran, J.-C.; Serp, P.; Kalck, P. *Inorg. Chem.* **2003**, *42*, 5523.

Table 1. ^{13}C and ^{1}H NMR Data and FAB/MS Values for the Ir and Pt Complexes Studied

Ir complex	^{13}C NMR (ppm)	^{1}H NMR (ppm)	IR (ν_{CO}, cm^{-1})	MS-FAB (*m/z*)
$[PPN][IrI_2(CO)_2]$ (**1-PPN**)	169.9 (s, CO)		2046 (vs), 1967 (s)	503
$[PPN][IrHI_3(CO)_2]$ (**2-PPN**)	155.0 (s, CO)	−11.65 (s, Ir-H)	2157 (w, ν_{IrH}) 2103 (s), 2052 (vs)	631
$[PPN][IrI_4(CO)_2]$ (**3-PPN**)	149.7 (s, CO)		2112 (s), 2068 (s)	
$[PPN][IrI_3(CH_3)(CO)_2]$ (**4-PPN**)	156.0 (s, CO); −16.6 (q, J_{C-H} = 141 Hz, CH_3)	2.15 (s, CH_3)	2100 (s), 2048 (s)	646
$H[IrI_3(CH_3)(CO)_2]$ (**4-H**)	157.1 (s, CO); −15.2 (q, J_{C-H} = 141 Hz, CH_3)			
$[IrI_2(CH_3)(CO)_2]_2$ (**5′**)	152.5, 150.4, 150.1 (s, CO); −5.3, −8.76 (q, J_{C-H} = 140 Hz, CH_3)	1.90, 1.85 (s, CH_3)	2120 (s), 2074 (s)	
$[IrI_2(CH_3)(CO)_3]$ (**6**)	146.9 (s); −22.3 (q, J_{C-H} = 140 Hz)	2.08 (s, CH_3)	2156 (s), 2116 (s), 2096 (s)	
cis-$[PPN][IrI_3(COCH_3)(CO)_2]$ (**8-PPN**)[a]	196.2 (s, *C*OCH_3); 151.4 (s, Ir−CO); 49.5 (s, CH_3*C*O)	3.13 (s, CH_3)	2111 (s), 2061 (s), 1679 (m), 1660 (m)	
trans-$[PPN][IrI_3(COCH_3)(CO)_2]$ (**8-PPN**)	201.5, (s, *C*OCH_3); 162.7 (s, Ir−CO); 52.2 (s, *C*H_3CO)	2.76 (s, CH_3)	2114 (w), 2070 (vs), 1655 (s)	
trans-$H[IrI_3(COCH_3)(CO)_2]$ (**8-H**)	203.4, (s, *C*OCH_3); 161.5 (s, Ir−CO); 50.6 (s, *C*H_3CO)	3.04 (s, CH_3)	2176 (w), 2115 (s), 1708 (m)	

other complexes	^{13}C NMR (ppm)	^{195}Pt and ^{1}H NMR (ppm)	IR (ν_{CO}, cm^{-1})	MS-FAB (*m/z*)
$H[PtI_3(CO)]$ (**9-H**)	156.8 (s, CO, J_{C-Pt} = 1649 Hz)	^{195}Pt: −5450 (J_{C-H} = 1649 Hz)	2068 (vs)	
$[PPN][PtI_3(CO)]$ (**9-PPN**)	152.8 (s, CO, J_{C-Pt} = 1759 Hz)	^{195}Pt: −5460 (J_{C-Pt} = 1759 Hz)	2075 (vs)	603
$[PtI_2(CO)]_2$ (**10'**)	154.5 (J_{C-Pt} = 1843 Hz)	^{195}Pt: −5328 (J_{C-Pt} = 1843 Hz)	2111 (vs)	
$[PtI_2(CO)_2]$ (**10**)	166.0 (J_{C-Pt} = 1466 Hz)	^{195}Pt: −5790 (J_{C-Pt} = 1466 Hz)	2127 (vs)	
$[PPN][Ir_2I_5(CH_3)_2(CO)_4]$ (**13-PPN**)	154.68 (s, CO); −14.83 (q, CH_3); J_{H-C} = 141 Hz	^{1}H: 2.28 (s, CH_3)	2117 (s), 2061 (s)	1161
$[PPN][IrI(CH_3)(CO)_2(\mu\text{-}I)_2PtI_2(CO)]$ (**11-PPN**)	155.4 (s, CO−Ir); 154.91 (s, CO−Pt, J_{Pt-C}= 1650 Hz); −14.09 (q, CH_3, J_{H-C}= 141 Hz); −14.18 (q, CH_3, J_{H-C} = 141 Hz)	^{1}H: 2.36 (s, CH_3) ^{195}Pt: −5462 (J_{Pt-C} = 1650 Hz)	2107 (s), 2050 (s)	1121

[a] See ref 16.

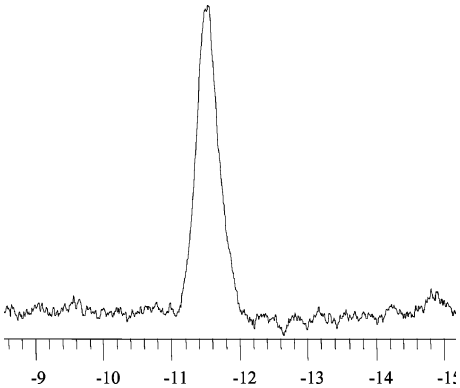

Figure 1. ^{1}H HP-NMR spectrum of complex **2-H** under preformation conditions (30 bar, 90 °C).

step in the iridium catalytic cycle is migratory CO insertion,[15] and the preliminary formation of the neutral pentacoordinated intermediate $[IrI_2(CH_3)(CO)_2]$ (**5**) is needed to account for that. Haynes et al. have demonstrated that iodide abstraction from **4** to afford **5** is favored by addition of methanol or a Lewis acid, such as InI_3.[16] Under dinitrogen, dimerization of **5** occurs and provides $[Ir_2(\mu\text{-}I)_2I_2(CH_3)_2(CO)_4]$ (**5′**), which has been characterized and gives, under CO, the tricarbonyl complex $[IrI_2(CH_3)(CO)_3]$ (**6**) (Scheme 1).[14,16] These authors, as Forster[12] did previously, have proposed that migratory CO insertion in **6** occurs readily under CO to give the neutral acyl species $[IrI_2(COCH_3)(CO)_3]$ (**7**). In a medium from which iodide ions had not been removed, the stable anionic complex $[IrI_3(COCH_3)(CO)_2]^-$ was isolated as the $[AsPh_4]^+$ salt **8-AsPh₄** and characterized as the fac,cis isomer.[10a] Theoretical studies show that the latter species is formed through kinetic control, while the trans isomer is the thermodynamic product.[17]

2.2. Stoichiometric Carbonylation of 4-PPN. By using a water/methanol mixture, we reacted $[PPN][IrI_3(CH_3)(CO)_2]$ (**4-PPN**) under 5 bar of CO and succeeded in obtaining and crystallizing the ***trans*-8-PPN** isomer. Its structure was determined by X-ray diffraction (Figure 3). The crystal structure of complex **8** with $AsPh_4^+$ as counterion was recently reported by Volpe et al.[18]

In the salt $[PPN][IrI_3(COCH_3)(CO)_2]$ (**8-PPN**) the anion adopts a trans geometry for the two CO ligands. The trans influence effect of the acetyl group is shown by the increased

(15) Pearson, J. M.; Haynes, H.; Morris, G. E.; Sunley, G. J.; Maitlis, P. M. *J. Chem. Soc., Chem. Commun.* **1995**, 1045.

(16) Ghaffar, T.; Adams, H.; Maitlis, P. M.; Sunley, G. J.; Baker, M. J.; Haynes, A. *Chem. Commun.* **1998**, 1023.

(17) (a) Kinnunen, T.; Laasonen, K. *J. Organomet. Chem.* **2001,** *628,* 222. (b) Kinnunen, T.; Laasonen, K. *J. Mol. Struct.* **2001**, *542*, 273.

(18) Volpe, M.; Wu, G.; Iretskii, A.; Ford, P. C. *Inorg. Chem.* **2006**, *45*, 1861.

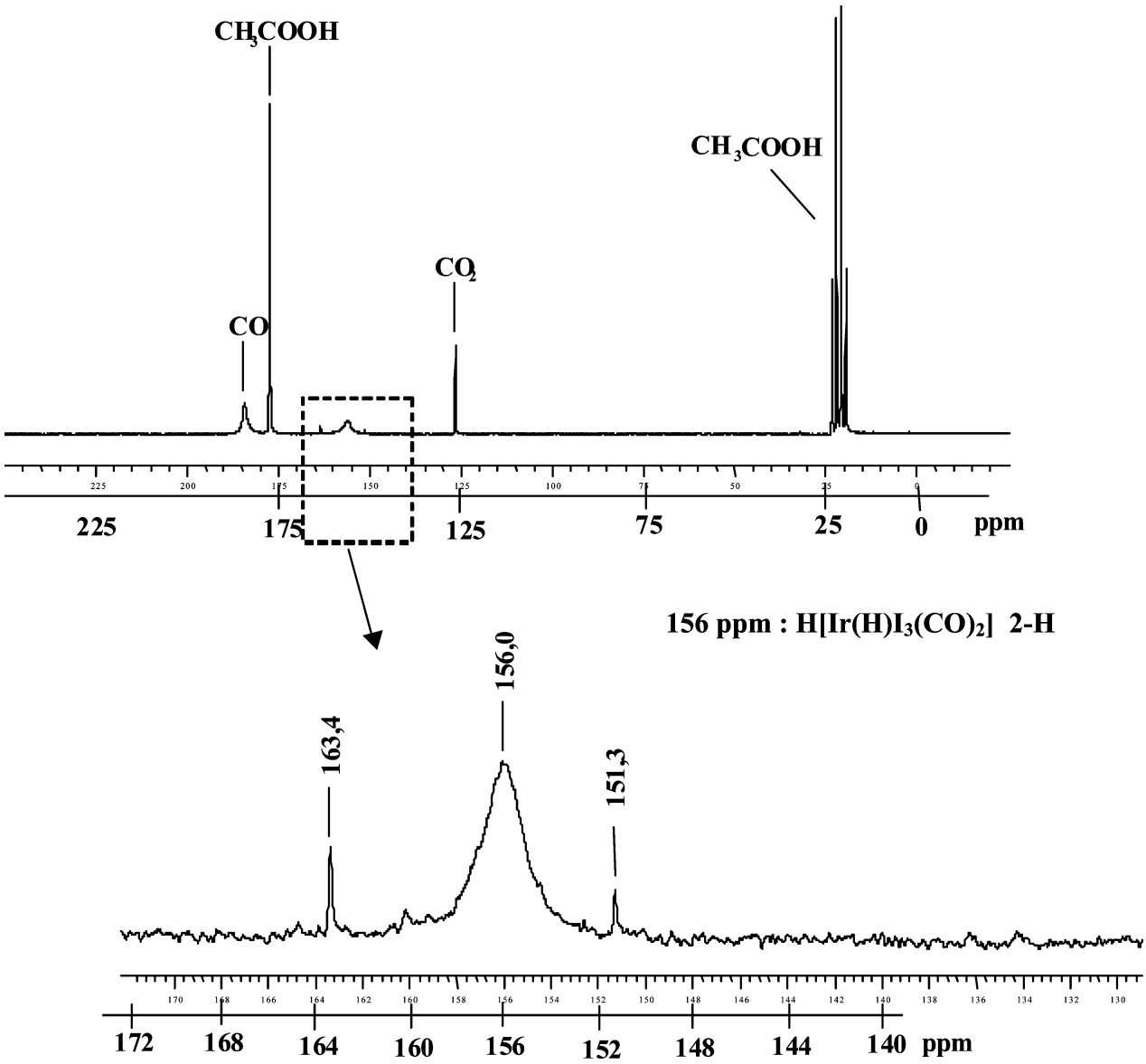

Figure 2. ^{13}C HP-NMR spectrum of a solution from preformation treatment (30 bar, 90 °C).

bond length of Ir(1)−I(2) = 2.8147(8) Å by comparison with the two other Ir−I bonds (ca. 2.70 Å). In addition, the C(4) carbon atom and the O(3) oxygen atom are approximately in the same plane as the Ir(1) and I(2) atoms and the two CO ligands. Most of the distances are in the same range as those for the fac,cis isomer,[10a] except for those in the acetyl ligand, in which the Ir−CO bond is longer for the cis isomer than for the trans one (2.058(12) Å). Indeed, all the other distances and angles shown by the present X-ray crystal structure fit well those observed for the cis isomer and are very close to those calculated by Kinnunen and Laasonen.[17] The compound ***trans*-8-PPN** was also characterized by IR and ^{13}C and ^{1}H NMR spectroscopy (Table 1).

By reacting [PPN][IrI$_3$(CH$_3$)(CO)$_2$] (**4-PPN**) with CO (5 bar, 1h, 25 °C) in a CH$_2$Cl$_2$/CH$_3$OH mixture, we produced mainly ***fac,cis*-8-PPN** instead (Figure 4a). Then we studied the effect of methanol concentration on the cis/trans ratio in this reaction and observed that the increase in the polarity and in the protic nature of the solvent plays a prominent role on this ratio. Indeed, we have seen by ^{1}H NMR, on the products isolated after reaction, that the addition of increasing quantities of methanol results in the production of higher amounts of the ***mer,trans*-8-PPN** isomer (signal at δ 2.77 ppm; see Figure 4). The signal at 3.60 ppm is due to traces of methanol presumably present in the crystal lattice, even after treatment in vacuo of the relevant **8-PPN** salts. Methanol would cause solvolysis of one iodide ligand followed by readdition of that very ligand, after a rearrangement process has occurred, thus giving the thermodynamic isomer. Moreover, worthy of note is that significant quantities of complex **4-PPN** (δ 2.18 ppm) are still seen in Figure 4a, which would also show that ***fac,cis*-8-PPN** is formed through kinetic control.

2.3. ^{13}C HP-NMR Experiments on the Catalytic Behavior of 1-H. We performed ^{13}C HP-NMR experiments under CO at high temperature, in the absence of any stabilizing counterion. The medium was the same as that used for our previous carbonylation batch experiments.[11]

^{13}C HP-NMR spectra reveal several carbonyl signals (Figure 5). First, the hydride complex **2-H**, which arises from WGSR, is still present, but the low intensity of its carbonyl signal at δ_C 156.4, as well as that of the signals due to carbon dioxide and **3-H,** all point to a small WGSR contribution. We can observe a rather intense signal at δ_C 157.1 ppm that, combined with the presence of a quartet at −15.2 ppm, indicates the presence of the methyl complex **4-H**. During a 4 h reaction we observed the progressive appearance of new signals at δ_C 203.4 (not

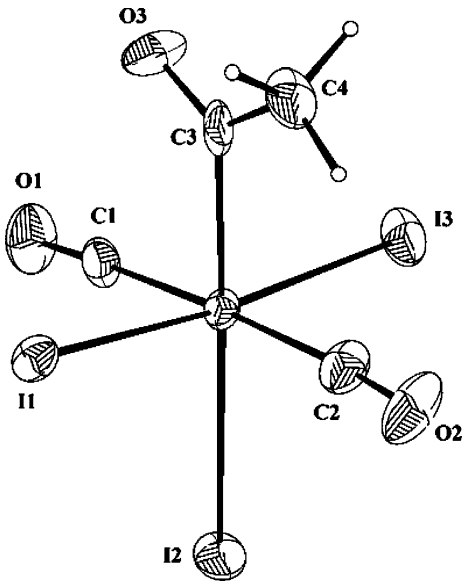

Figure 3. Ortep diagram of $[PPN][IrI_3(COCH_3)(CO)_2]$ (***mer,trans*-8-PPN**). The PPN^+ counterion is omitted for clarity purposes. Ellipsoids are at the 50% probability level. Selected bond lengths (Å): Ir(1)−I(1) = 2.6849(8), Ir(2)−I(2) = 2.8147(8), Ir(1)−I(3) = 2.6984(9), Ir(1)−C(1) = 1.929(11), Ir(1)−C(2) = 1.915(13), Ir(1)−C(3) = 2.058(12), C(1)−O(1) = 1.116(13), C(2)−O(2) = 1.104(14), C(3)−O(3) = 1.183(14), C(3)−C(4) = 1.487(18). Selected bond angles (deg): I(1)−Ir(1)−I(2) = 91.85(3), I(1)−Ir(1)−I(3) = 174.65(3), I(2)−Ir(1)−I(3) = 93.07(3), I(1)−Ir(1)−C(1) = 89.8(3), I(2)−Ir(1)−C(1) = 89.8(3), I(3)−Ir(1)−C(1) = 88.1(3), I(1)−Ir(1)−C(2) = 91.6(4), I(2)−Ir(1)−C(2) = 86.1(3), I(3)−Ir(1)−C(2) = 90.8(4), C(1)−Ir(1)−C(2) = 175.7(5), I(1)−Ir(1)−C(3) = 87.4(3), I(2)−Ir(1)−C(3) = 178.3(3), I(3)−Ir(1)−C(3) = 87.7(3), C(1)−Ir(1)−C(3) = 88.7(5), C(2)−Ir(1)−C(3) = 95.5(5), Ir(1)−C(1)−O(1) = 177.8(11), Ir(1)−C(2)−O(2) = 175.4(12), Ir(1)−C(3)−C(4) = 117.9(9), Ir(1)−C(3)−O(3) = 119.9(9), C(4)−C(3)−O(3) = 122.0(12).

shown), 161.7, and 50.6 ppm (Figure 5), which correspond to the anionic acyl species ***trans*-8-H**. This observation confirms that the slowest step in the iridium-catalyzed methanol carbonylation is CO migratory insertion, affording **8-H**.

3. Platinum Cocatalyst Activity. 3.1. Characterization and Role of the Species Formed under Dinitrogen at Ambient Temperature. We studied the promoting effect of $[PtI_2(CO)]_2$ by employing a model system based on the use of PPN^+ salts of the relevant Ir anions and by running experiments under dinitrogen at ambient temperature, with CH_2Cl_2 as solvent. Addition of $[PtI_2(CO)]_2$ (**10′**) during the catalytic runs dramatically enhances the reaction rate. We have checked the activity of the compound itself and observed that it does not catalyze methanol carbonylation. Hence, the increased activity can be attributed to the direct involvement of the carbonyliodoplatinum dimer in the CO migratory insertion step.

In order to elucidate its role as promoter, addition of labeled $[PtI_2(^{13}CO)]_2$ (**10′**) to a dichloromethane solution of the labeled salt $[PPN][IrI_3(CH_3)(^{13}CO)_2]$ (**4-PPN**) (Pt/Ir = 0.3/1) was conducted under dinitrogen. The room-temperature reaction is instantaneous, and the ^{195}Pt NMR spectra reveal two signals at −5460 and −5462 ppm. The signal at −5460 ppm (d, $J^{13}C-^{195}Pt$ = 1759 Hz) corresponds to the salt $[PPN][PtI_3(CO)]$ (**9-PPN**) (Figure 6), which we have characterized independently by X-ray diffraction.

By a separate synthesis, suitable crystals of **9-PPN** were obtained by reacting the dimeric species $[PtI_2(CO)]_2$ with HI, followed by addition of [PPN]Cl under dinitrogen. In this

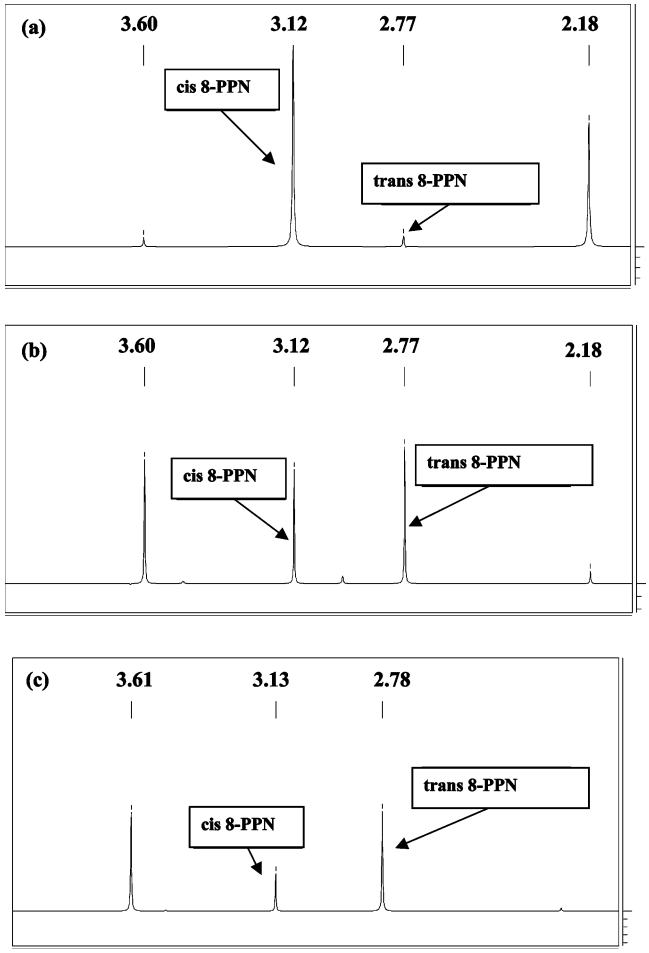

Figure 4. ^1H NMR spectra showing the variation in the amounts of the cis/trans acyl species resulting from three separate carbonylation experiments on **4-PPN**, performed at different CH_2Cl_2/CH_3OH ratios: (a) CH_2Cl_2/CH_3OH 35 mL/5 mL; (b) CH_2Cl_2/CH_3OH 20 mL/20 mL; (c) CH_2Cl_2/CH_3OH 5 mL/35 mL.

compound the anion presents a distorted-square-planar geometry (Figure 7), with a very small trans influence of the carbonyl ligand.[19]

The second peak at −5462 ppm (d, $J^{13}C-^{195}Pt$ = 1650 Hz) can be assigned to the heterobimetallic compound $[PPN][IrI_2(CH_3)(CO)_2(\mu\text{-}I)PtI_2(CO)]$ (**11-PPN**), in which the anion has a structure with one iodide bridge. A diiodo-bridged structure could also be hypothesized, involving a five-coordinate platinum center, but as Pt(II) preferentially adopts a square-planar geometry, the former isomeric form would be the preferred one. The subsequent cleavage by CO of this anionic species would accelerate the slowest step in the iridium catalytic cycle, providing the iridium neutral species **6**, within which methyl cis migration is favored under CO (Scheme 2). Indeed, **11-PPN** is detected at room temperature in CH_2Cl_2 solution upon instantaneous reaction of the promoter with the **4-PPN** salt.

Although the major role played by the promoter in abstracting an iodide ligand from **4-PPN** via the intermediate formation of **11-PPN** is evident under model conditions, another important aspect of its behavior under operating catalytic conditions should not be disregarded: $[PtI_2(CO)]_2$ could also act as scavenger of the I^- ions released by Ir−I bond rupture at elevated temperature in polar/coordinating solvents, thus moderating[10a] their concen-

(19) Hartley, F. R. In *Comprehensive Organometallic Chemistry*; Wilkinson, G., Stone, F. G. A., Abel, E. W., Eds.; Pergamon Press: Oxford, U.K., 1982; p 490.

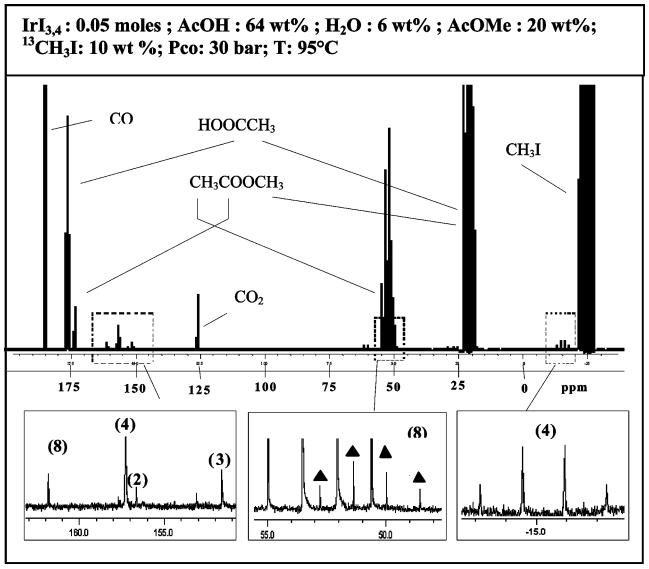

Figure 5. ^{13}C HP-NMR spectra of solutions from batch experiments on the Ir-catalyzed methanol carbonylation.

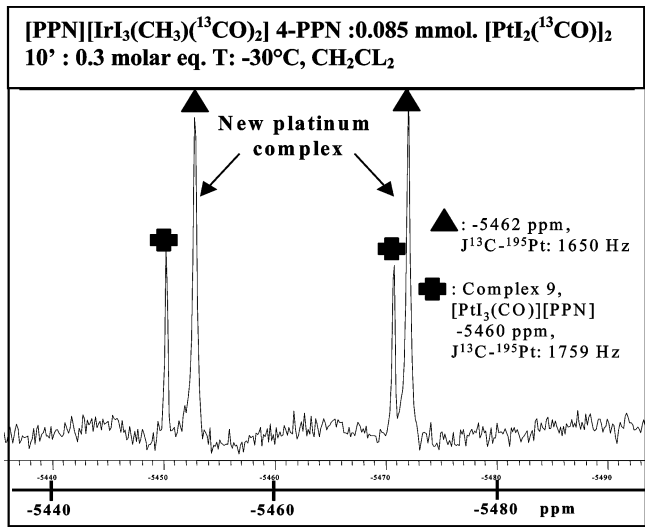

Figure 6. Platinum species identification by ^{195}Pt NMR spectroscopy.

tration in solution to aid the displacement of iodide by CO in $[IrI_3(CH_3)(CO)_2]^-$, with generation of the neutral species $[IrI_2(CH_3)(CO)_3]$.

^1H NMR spectra of the aforementioned reaction solution showed the formation of the dimer $[Ir_2(\mu\text{-}I)_2I_2(CH_3)_2(CO)_4]$ (**5′**), of the salt [PPN][$IrI_2(CH_3)(CO)_2(\mu$-I)$PtI_2(CO)$] (**11-PPN**), of the complex $[IrI_2(CH_3)(CO)_2(solv)]$ (**12**), and of [PPN][$Ir_2I_4(\mu$-I)$(CH_3)_2(CO)_4$] (**13-PPN**). To assign all of the relevant signals, we studied the changes in their relative intensities by varying the concentrations of **10′** and **4-PPN**: signals at 2.36, 2.28, 2.14, 2.09, 1.90, and 1.85 ppm were observed (Figure 8). The signal at 2.14 ppm corresponds to unreacted **4-PPN** and presents a significant intensity even at low Pt/Ir molar ratios. The signal at 2.09 ppm could be attributed to the pentacoordinated, or hexacoordinated solvated, neutral species $[IrI_2(CH_3)(CO)_2(solv)]$ (**12**), "solv" being presumably either a CD_2Cl_2 molecule, since $Ir-CH_2Cl_2$ complexes are known,[20] or H_2O present as traces in the solvent. Such attribution can indeed be made in view of the concomitant presence (see below) of the dimer $[Ir_2I_2(\mu\text{-}I)_2(CH_3)_2(CO)_4]$ (**5′**), which is likely to form from **12** in weakly coordinating solvents.

(20) Crabtree, R. H. In *The Organometallic Chemistry of the Transition Metals*; 3rd ed.; Wiley-Interscience: New York, 2001; p 109.

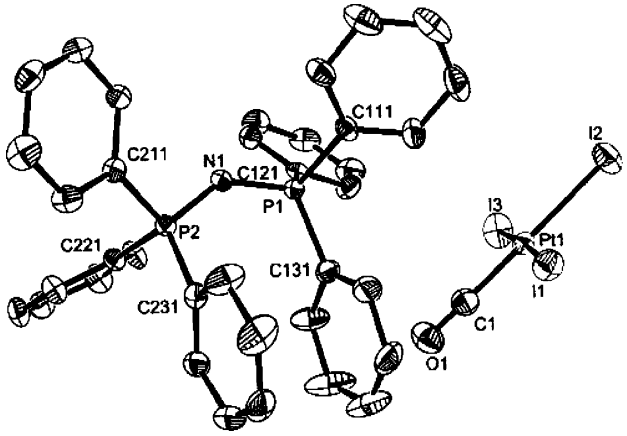

Figure 7. Ortep diagram of [PPN][$PtI_3(CO)$] (**9-PPN**). Ellipsoids are at the 50% probability level. Selected bond lengths (Å): Pt(1)−C(1) = 1.822(8), Pt(1)−I(1) = 2.6068(4), Pt(1)−I(2) = 2.6110(4), Pt(1)−I(3) = 2.6127(5), C(1)−O(1) = 1.135(7). Selected bond angles (deg): C(1)−Pt(1)−I(1) = 87.54(18), C(1)−Pt(1)−I(2) = 179.33(18), C(1)−Pt(1)−I(3) = 88.57, I(1)−Pt(1)−I(2) = 92.402(15), I(1)−Pt(1)−I(3) = 176.017, I(2)−Pt(1)−I(3) = 91.494(16), O(1)−C(1)−Pt(1) = 178.6(6).

Scheme 2. Schematic Pathway Showing the Reaction of 10′ with 4

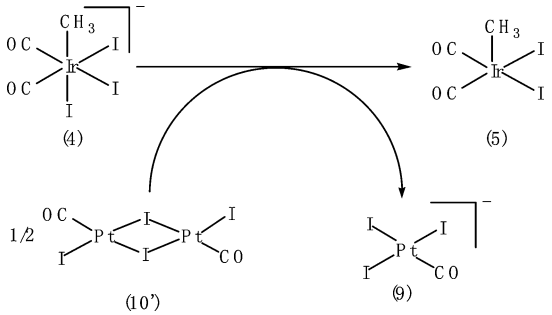

The two signals at 1.90 and 1.85 ppm increase simultaneously at high Pt/Ir molar ratios (1/1.8), pointing to the formation of the two isomers of the neutral homobimetallic dimer **5′**.[14] As for the two signals at 2.36 and 2.28 ppm, we observed that their relative intensities varied with the Pt/Ir molar ratio. Hence, we recorded for every each Pt/Ir value the ^1H NMR spectrum in tandem with its FAB/MS spectrum. As shown in Figure 9, two anionic complexes were detected at *m*/*z* 1121 and 1161, respectively. For a relatively high platinum to iridium ratio of 1/2.65, we observed that the signal at 2.36 ppm in the ^1H NMR spectrum increases simultaneously with the peak at *m*/*z* 1121 in the FAB/MS, pointing to the presence of the compound **11-PPN**. For a lower Pt/Ir ratio of 1/4.75 the signal at *m*/*z* 1121 almost completely disappears from FAB/MS, as well as the ^1H NMR signal at 2.36 ppm, so that the two signals at 2.28 ppm and *m*/*z* 1161 can be unambiguously attributed to **13-PPN**. It turns out that this monoiodo-bridged anionic diiridium species and the dimer proposed as a possible intermediate in the Ir−Ru system[9] are one and the same.

We also recorded ^1H and ^{13}C NMR spectra of the same reaction mixtures in order to assign the ^{13}C signals (Table 1). Figure 10 shows two examples relevant to two different Pt/Ir molar ratios (1/2.65 and 1/4.75, respectively). We compared the variations in the ^1H NMR signals to those in the ^{13}C signals. Thus, we could note that the intensity of the peak at 2.36 ppm, attributed to the compound **11-PPN**, varies in the same way as

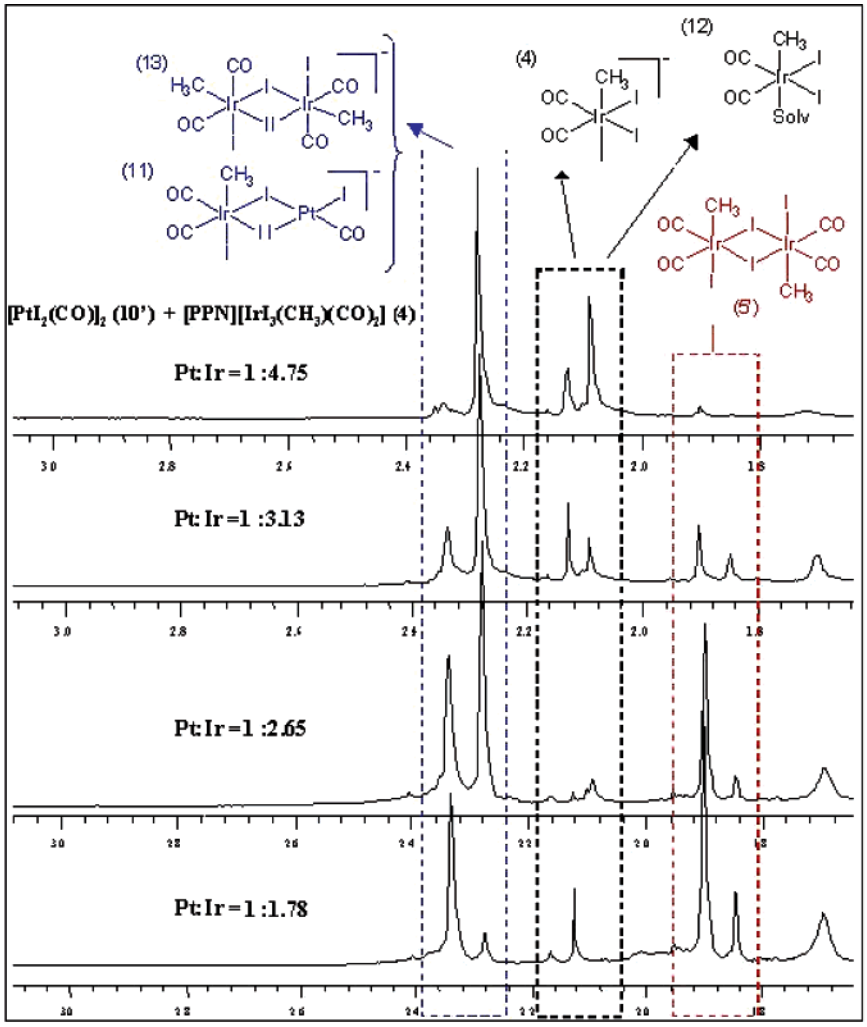

Figure 8. [1] H NMR studies showing the influence of the Pt/Ir ratio on the nature of the species observed in the reaction of **10′** with **4-PPN.**

that of the two CO peaks at 155.41 and 154.94 ppm. Owing to the presence of the two ^{195}Pt satellites (not shown in Figure 10 for clarity purposes), we assigned the signal at 154.94 ppm to the CO ligand bound to the platinum center; thus, the signal at 155.41 ppm was attributed to the two CO ligands coordinated to iridium. Similarly, the signal at 155.56 ppm, present only at lower Pt/Ir molar ratios, is assigned to unreacted **4-PPN**, and the ^{13}C NMR signal at 154.69 ppm, related to the ^{1}H NMR signal at 2.28 ppm, can be associated with the dimer **13-PPN**. From the ^{13}C NMR spectrum in Figure 10b the presence of **9-PPN** (152.75 ppm) is evident, as well as that of **5′** (152.14, 150.00, 149.68 ppm).

Hence, from the identification of the various species produced by reaction of **10′** with **4** we can propose the mechanistic pathway depicted in Scheme 3. The anionic monoiodo-bridged [Ir−Pt] heterobimetallic species **11** is possibly an intermediate through which the platinum promoter exerts its role as iodide abstractor and accelerating agent.

3.2. ^{1}H HP-NMR Experiments on the Reaction between 10′ and the Ir Species Formed by Carbonylation of 1-H. We were also interested in elucidating the reactivity under CO of H[$IrI_2(CO)_2$] (**1-H**) in the presence of the Pt cocatalyst to compare the HP-NMR results to those obtained using **1-H** alone.

A sapphire tube was charged with IrI_3/IrI_4 and [$PtI_2(CO)]_2$ (Pt/Ir = 1/4) in CH_3COOH (64 wt %), CH_3COOCH_3 (20 wt %), H_2O (6 wt %), and labeled $^{13}CH_3I$ (10 wt %) and then pressurized under 30 bar of ^{12}CO/^{13}CO and heated to 86 °C. By ^{13}C NMR spectroscopy we compared the intensity of the acetic acid and iodomethane signals and, in particular, their ratios. We could reasonably make such a comparison, since the iodomethane formed during the carbonylation is not labeled, so that the signal observed does actually decrease only when labeled iodomethane (i.e., the reactant) is consumed. We observed, for the same reaction times (20 min), that the Ir−Pt system leads to the consumption of larger amounts of $^{13}CH_3I$ than does the Ir system (Figure 11). We also noted the formation of $^{13}CO_2$ (125.0 ppm) and $^{13}CH_4$ (−4.2 ppm, quintet) as byproducts (Figure 12). As for the formation of iridium or platinum species, we detected **4-H** (Figure 12), identified as the major product, together with **8-H** and **9-H**, the presence of the last compound being confirmed by ^{195}Pt NMR. We also observed that under 30 bar of CO the monomer [$PtI_2(CO)_2$] (**10**), which is the stable carbonyliodoplatinum species formed by [$PtI_2(CO)]_2$ under carbon monoxide, is regenerated from H[PtI_3-(CO)] in the presence of a HI scavenger (molecular sieves).

Thus, it appears that the role of the platinum promoter is to abstract iodide from the methyliridium complex **4-H** via a monoiodo-bridged species and/or to scavenge iodide ions coming from rupture of Ir−I bonds under more drastic conditions. Under CO such a Ir−Pt dimer undergoes rapid cleavage to give the neutral methyltricarbonyliridium complex [$IrI_2(CH_3)$-$(CO)_3$] (**6**). Then migratory CO insertion occurs within this active intermediate to produce the neutral coordinatively unsaturated species [$IrI_2(COCH_3)(CO)_2$] (**7**), from which

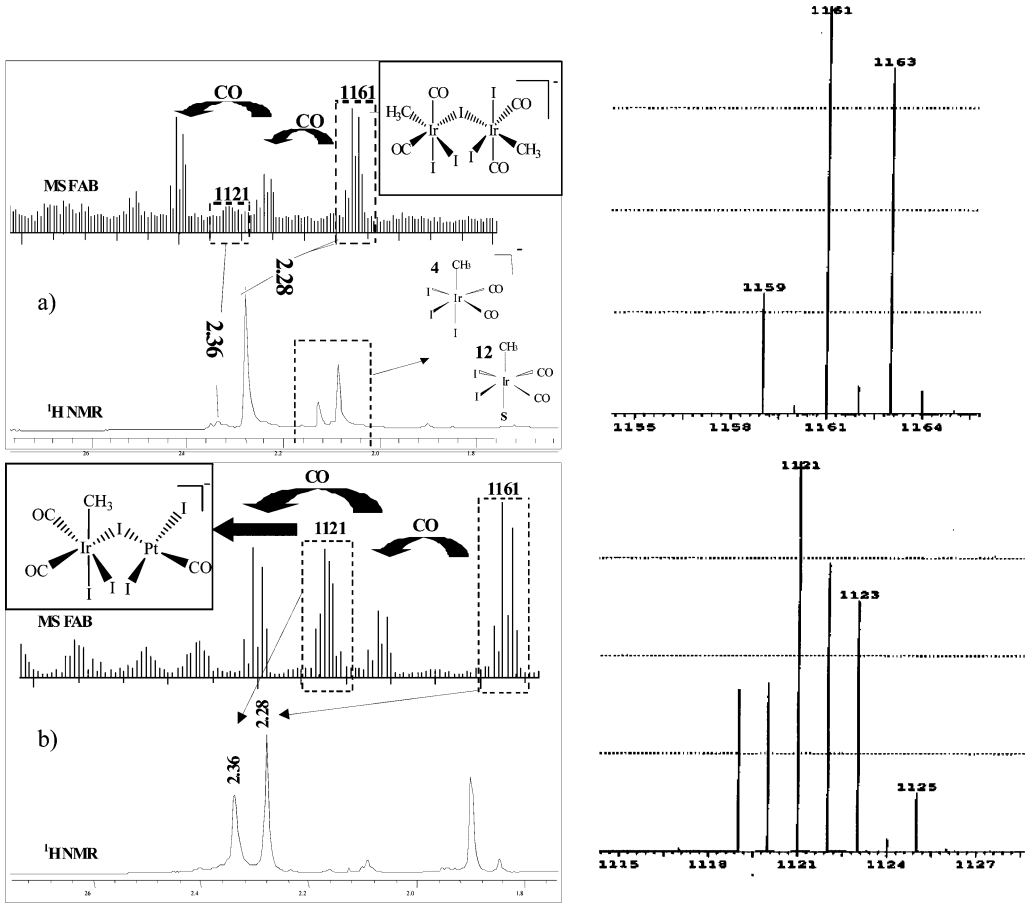

Figure 9. Correlations between FAB-MS and ^{1}H NMR spectra for the reaction of **10′** with **4-PPN**: at Pt/Ir = 1/4.75 (a) and at Pt/Ir = 1/2.65 (b). Comparisons with calculated mass spectra are shown to the right.

$[IrI_3(COCH_3)(CO)_2]^-$ (**8**) is formed by subsequent coordination of an iodide ion. On the basis of the evidence found by employing a model system, we tentatively propose the catalytic cycle shown in Scheme 4, which also highlights another possible pathway involving the mononuclear unsaturated species **5**.

In Scheme 4 the interconnected platinum cycle is also depicted. Compound **9-H**, which has been observed by IR and NMR, is directly formed by cleavage of **11-H**, slowly regenerating **10** by substitution of CO for iodide. The species detected by HP-NMR are shown in boldface characters in the catalytic cycle.

We have included the water-gas shift reaction, which involves the protonated species **1-H**, **2-H**, and **3-H**. With regard to the amounts of methane found, it may arise from the reaction of CH_3I with **2-H**, as shown in the cycle, but also from the reaction between **4-H** and HI.

Conclusion

In this study we have shown that $[PtI_2(CO)]_2$ exerts a promoting effect on the catalytic activity of the Ir-based methanol carbonylation to acetic acid. The role of the promoter is to abstract an iodide ligand by reaction with the anionic resting state $[IrI_3(CH_3)(CO)_2]^-$ and/or to scavenge iodide ions released in solution. Under model conditions, a heterobimetallic complex, which could be considered as an intermediate, has been detected and characterized by coupled NMR and FAB/MS; then, under CO, this anionic monoiodo-bridged [Ir−Pt] species undergoes cleavage to $[PtI_3(CO)]^-$ and $[IrI_2(CH_3)(CO)_3]$, the latter producing an acyl species and then acetyl iodide, which is in turn hydrolyzed to acetic acid.

In summary, we propose the intermediacy of $[IrI_2(CH_3)(CO)_2$-$(\mu$-I$)PtI_2(CO)]^-$ on the basis of all the experimental data we have obtained; however, the possible intervention of mononuclear species and iodide transfer from Ir to Pt by a stepwise dissociation/coordination mechanism would provide an alternative pathway for the promoting effect of carbonyliodoplatinum species under operating conditions.

Experimental Section

1. Materials. All reactions and manipulations of Ir and Pt complexes were performed under an argon or dinitrogen atmosphere. Dichloromethane was distilled using CaH_2. Other reagents were used as supplied: the salt IrI_3/IrI_4, denoted $IrI_{3,4}$ (Johnson-Matthey), platinum(II) iodide, bis(triphenylphosphoranylidene) chloride ([PPN]Cl), ^{13}C-labeled methyl iodide, and triphenylphosphine (Aldrich), acetyl chloride, methyl iodide, and indium triiodide (Acros), acetone, acetic acid, chlorobenzene, chloroform, dichloromethane, dimethylformamide, *n*-hexane, *n*-heptane, methanol, *n*-pentane, and toluene (Scharlau), chloroform-d_3, dichloromethane-d_2, methanol-d_4, and toluene-d_8 (Eurisotop), argon, dinitrogen, carbon monoxide, and ^{13}C-labeled carbon monoxide (Air Liquide), and hydriodic acid (Merck). Labeling experiments were performed by stirring the relevant dissolved complex under a ^{13}CO atmosphere for a few hours.

2. Instrumentation. IR spectra were recorded on a Perkin-Elmer 1710 Fourier Transform spectrophotometer using either a solution cell with CaF_2 windows or CsI salt for solid pellet analysis. ^{1}H, ^{13}C, and ^{195}Pt NMR spectra were recorded on a Bruker AC250 or on a AMX400 spectrometer. Mass spectra were recorded by the negative FAB method on a NERMAG R10-10 mass spectrometer.

X-ray crystallographic data for the compounds **8-PPN** and **9-PPN** were collected on an Oxford-Diffraction Xcalibur diffractometer. Final unit cell parameters were obtained by the least-squares

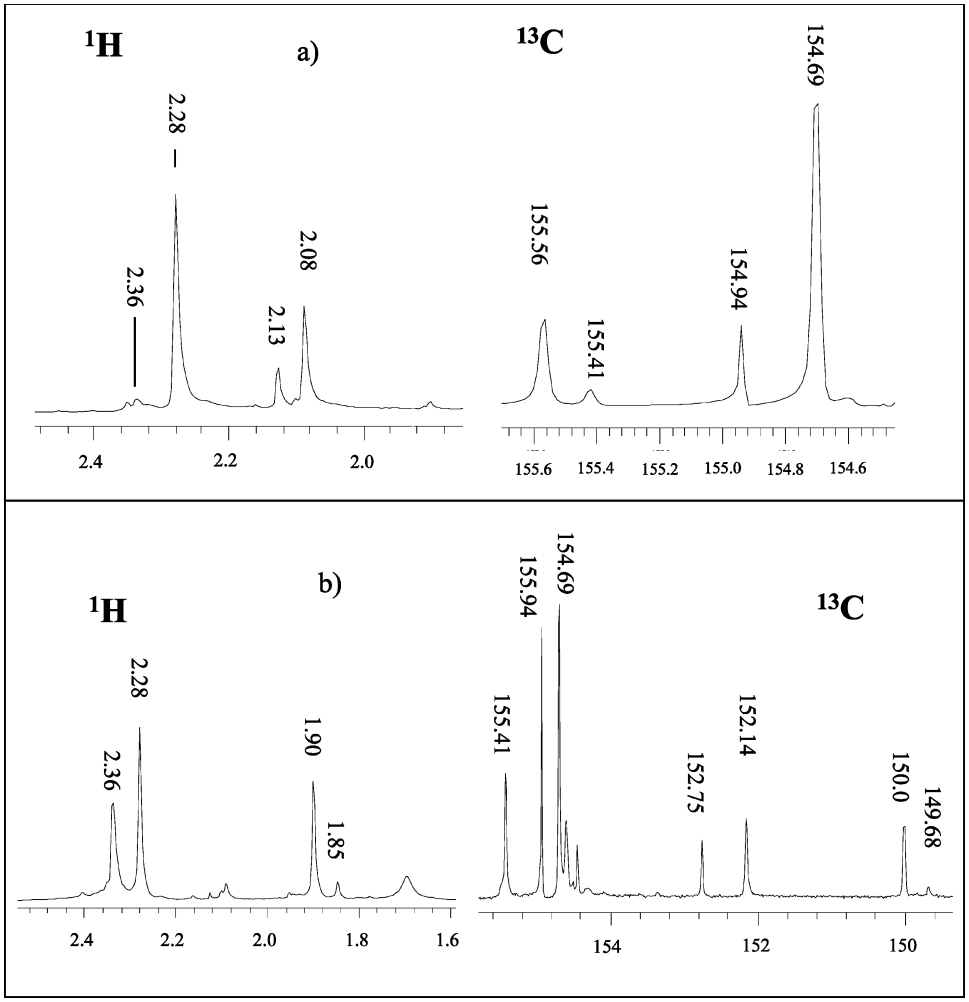

Figure 10. Correlations between ^{1}H and ^{13}C spectra for the reaction of **10′** with **4-PPN**: (a) Pt/Ir = 1/4.75; (b) Pt/Ir = 1/2.65.

Scheme 3. Iodide Abstraction Pathway

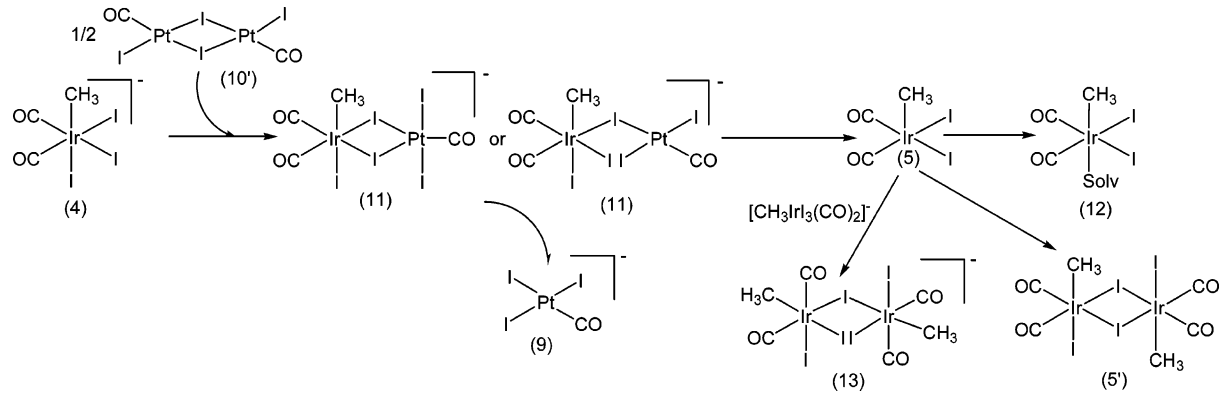

refinement of a large number of selected reflections. Structures were solved by direct methods (SIR97)[21] and refined by least-squares procedures either on F^2 using SHELXL-97[22] for **9-PPN** or on F using CRYSTALS[23] for **8-PPN**. In all of the compounds, all H atoms were introduced at calculated positions as riding atoms (d(CH) = 0.99−0.98 Å) with a displacement parameter equal to 1.2 (C_6H_5) or 1.5 (CH_3) times that of the parent atom.

Calculations were carried out with the SHELXL-97 program using the integrated system WINGX (version 1.63)[24] or the CRYSTALS package. Molecular views were obtained with the help of ORTEPIII[25] or CAMERON.[26] Fractional atomic coordinates, anisotropic thermal parameters for non-hydrogen atoms, and atomic coordinates for H atoms have been deposited with the Cambridge Crystallographic Data Center. Copies of the data can be obtained free of charge on application to the Director, CCDC, 12 Union Road, Cambridge CB2 IE2, U.K.

(21) Altomare, A.; Burla, M. C.; Camalli, M.; Cascarano, G. L.; Giacovazzo, C., Guagliardi, A.; Moliterni, A. G. G.; Polidori, G.; Spagna, R. SIR97-a program for automatic solution of crystal structures by direct methods. *J. Appl. Crystallogr.* **1999**, *32*, 115.

(22) Sheldrick, G. M. SHELXL97: Program for Crystal Structure Refinement; University of Göttingen, Göttingen, Germany, 1997.

(23) Betteridge, P. W.; Carruthers, J. R.; Cooper, R. I.; Prout, K.; Watkin, D. J. *J. Appl. Crystallogr.* **2003**, *36*, 1487.

(24) Farrugia, L. J. WinGX. *J. Appl. Crystallogr.* **1999**, *32*, 837.

(25) Farrugia, L. J. ORTEP-3 for Windows, *J. Appl. Crystallogr.* **1997**, *30*, 565.

(26) Watkin, D. J.; Prout, C. K.; Pearce, L. J. CAMERON; Chemical Crystallography Laboratory, Oxford, U.K., 1996.

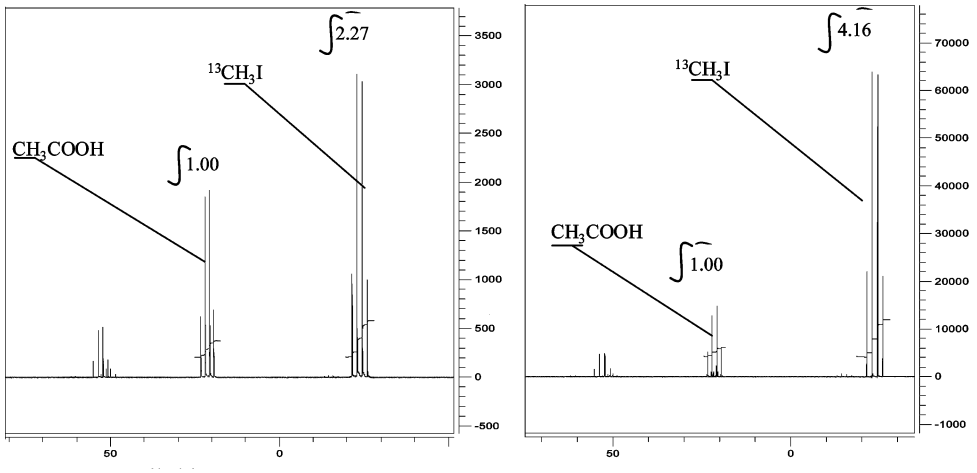

Figure 11. Comparison of the CH_3COOH/CH_3I ratio between the Ir−Pt system (left) and that of Ir alone (right).

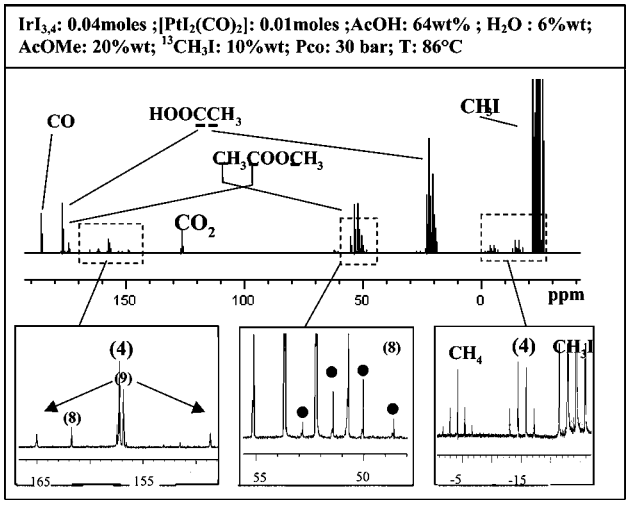

Figure 12. ^{13}C NMR spectra for the Ir−Pt-catalyzed methanol carbonylation.

3. Batch Experiments. High-pressure batch carbonylation experiments were performed in a Hastelloy B2 100 mL autoclave (Top Industrie) equipped with a stirring axis. The reactor can be pressurized up to 90 bar from a gas reservoir and can be heated up to 200 °C. Pressure can be maintained in the reactor. We measured carbon monoxide consumption in the reservoir and then calculated the carbonylation rate at 20% of unreacted methyl acetate. The reactor is equipped with a feed line to introduce liquids under pressure. All batch experiments were started with the $IrI_{3,4}$ salt in a mixture of acetic acid and water (10/1); the reactor was closed and flushed several times with carbon monoxide and then pressurized at 5 bar and heated to 190 °C, and the mixture was stirred at 1000 rpm to preform the iridium active species. After 25 min, $[PtI_2(CO)]_2$ was dissolved in the liquid component and added through the liquid feed line overpressurized with carbon monoxide. The pressure was then adjusted to 30 bar. It can be maintained constant by supplying gas from the reservoir during the experiments. A glassware reactor (Top Industrie) was used for some experiments. Technical features and working conditions were the same as those used for the Hastelloy autoclave, except for the maximum operating pressure, which was 8 bar. With such a reactor it was possible to observe the reaction mixture during the experiments and perform crystallizations afterward.

4. High-Pressure/High-Temperature IR Analyses. Batch experiments were monitored in situ by high-pressure IR spectroscopy in an autoclave equipped with a cylindrical internal reflectance (CIR) silicon rod: a "Cassegrain" lens system was used to focus the IR beam onto the rod placed across a Hastelloy B2 (Top Industrie) batch 100 mL autoclave and to refocus the IR beam onto the detector. Spectra were recorded on a Perkin-Elmer GXII spectrophotometer. The reactor can be pressurized up to 50 bar with CO and heated up to 200 °C. A solution can be added into the reactor under pressure using a liquid feed line.

5. High-Pressure NMR Analyses. Batch carbonylation experiments were monitored in situ by high-pressure NMR spectroscopy using sapphire tubes (10 mm e.d.), pressure rated to 100 bar, fitted with a titanium valve. Reaction mixtures can be heated up to 100 °C.

All high-pressure NMR experiments were performed on a Bruker DRX400 spectrometer. The NMR tube was charged with $IrI_{3,4}$, $[PtI_2(CO)]_2$, and the reaction mixture. Once the tube was sealed, the medium was flushed several times with ^{12}CO and then pressurized to 10 bar with ^{13}CO. The pressure was then adjusted to 30 bar with ^{12}CO.

6. Synthesis of Iridium Compounds. 6.1. [PPN][$IrI_2(CO)_2$] (1-PPN). This compound was prepared from $IrI_{3,4}$ (2 g, 3.21 mmol) in a mixture of DMF (150 mL) and water (1.5 mL). The solution was stirred under a gentle CO bubbling at 160 °C for 3 h. The initially dark red solution turned yellow due to the presence of $[NH_2Me_2][IrI_2(CO)_2]$. [PPN]Cl (1.84 g, 3.21 mmol) was then added, and the solution was cooled to room temperature. Cold water (750 mL, 1−3 °C) was then slowly added in order to precipitate $[PPN][IrI_2(CO)_2]$ (**1-PPN**). The yellow powder was filtered and washed three times with 50 mL of cold water. This product was dried under vacuum and crystallized at −18 °C in a bilayered mixture of CH_2Cl_2 and *n*-hexane (1/1). After a few hours yellow needle-shaped crystals were obtained (2.67 g, 80%). IR (CH_2Cl_2): ν(CO)/cm^{-1} 2046, 1967. IR (CsI): ν(CO)/cm^{-1} 2045, 2034, 1968, 1960. $^{13}C\{^1H\}$ NMR (CD_2Cl_2): δ 169.9 (Ir−CO). MS (FAB^-): *m*/*z* 503. Anal. Calcd for $C_{38}H_{30}IrI_2NO_2P_2$: C, 43.86; H, 2.91; N, 1.35. Found: C, 43.69; H, 2.81; N, 1.38.

6.2. [PPN][$IrHI_3(CO)_2$] (2-PPN). This compound was prepared from $[PPN][IrI_2(CO)_2]$ (**1-PPN**; 0.5 g, 0.48 mmol) dissolved in 20 mL of dichloromethane by dropwise addition of HI (57% in water, 0.1077 g, 0.48 mmol). The slow addition of HI was monitored by IR, and after a few minutes CO bands corresponding to [PPN][Ir(H)$I_3(CO)_2$] (**2-PPN**) were observed, while those corresponding to **1-PPN** had completely disappeared. The solvent was then removed under vacuum, and an orange-red solid was obtained. This product was crystallized in an acetone/*n*-heptane (1/1) bilayered mixture to afford small reddish orange crystals (0.55 g, 98%) not suitable for X-ray analysis. IR (CH_2Cl_2): ν(CO)/cm^{-1} 2157, 2103, 2052. ^1H NMR (CD_2Cl_2): δ −11.7 (s, H−Ir). $^{13}C\{^1H\}$ NMR (CD_2Cl_2): δ 155.0 (s, Ir−CO). MS (FAB^-): *m*/*z* 631. Anal. Calcd for $C_{38}H_{31}IrI_3NO_2P_2$: C, 39.06; H, 2.67; N, 1.20. Found: C, 39.21; H, 2;63; N, 1.22.

Scheme 4. Proposed Catalytic Cycle for the Ir−Pt-Catalyzed Methanol Carbonylation

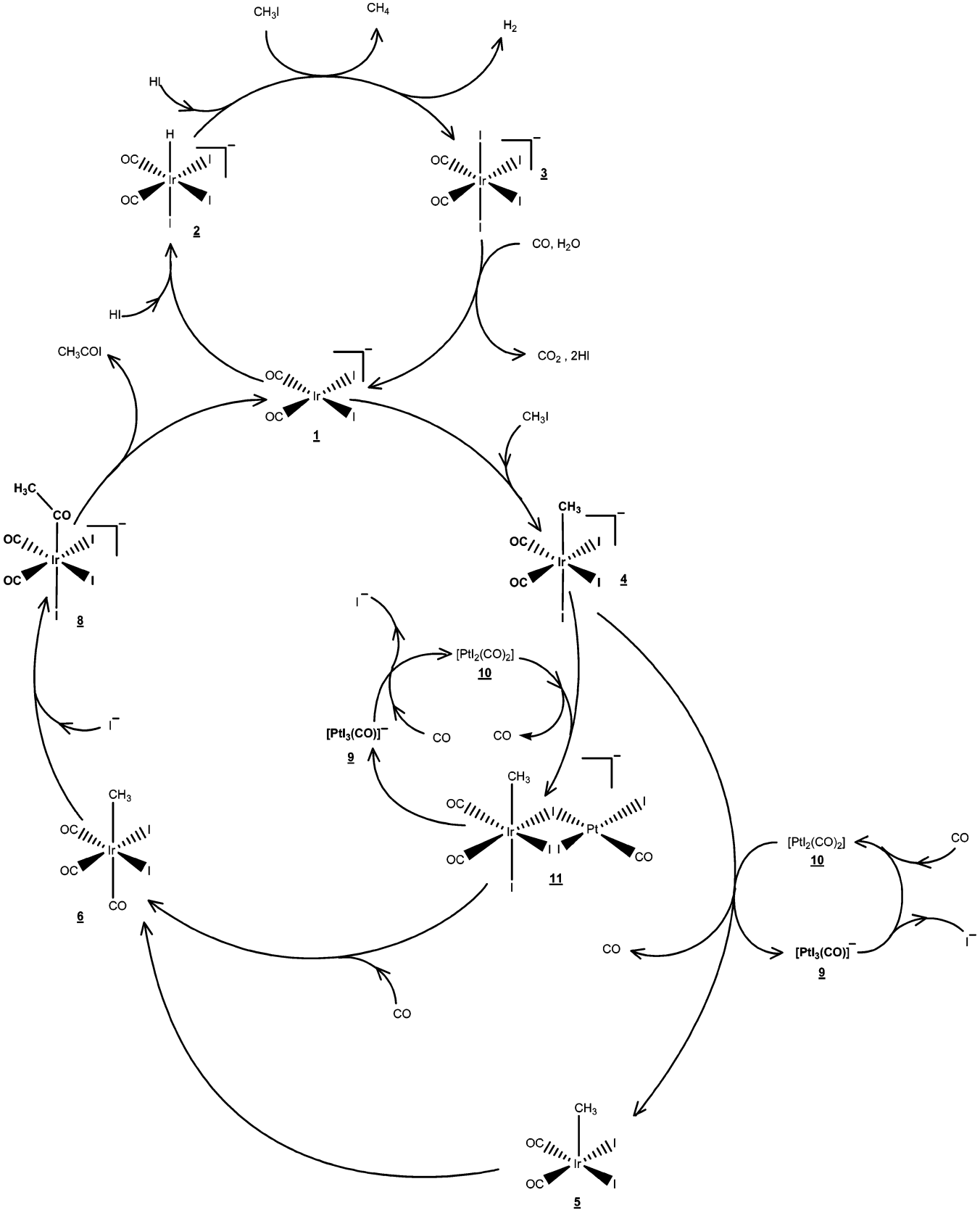

6.3. [PPN][IrI$_4$(CO)$_2$] (3-PPN). The salt [PPN][IrI$_2$(CO)$_2$] (1 g, 0.96 mmol) was dissolved in 50 mL of dichloromethane, and iodine (0.24 g, 0.96 mmol) was added to the solution. The mixture was stirred for 10 min, and then the solvent was removed under vacuum to obtain a red powder (1.01 g, 80%). IR (CH_2Cl_2): ν(CO)/cm^{-1}: 2112, 2068. $^{13}C\{^1H\}$ NMR (CD_2Cl_2): δ 149.7 (s, Ir−CO).

6.4. [PPN][IrI$_3$(CH$_3$)(CO)$_2$] (4-PPN). This compound was prepared by starting from [PPN][IrI$_2$(CO)$_2$] (1 g, 0.96 mmol) dissolved in 10 mL of dichloromethane. Methyl iodide (5.45 g,

38.4 mmol) was added to the medium, and the solution was stirred at room temperature for 1 h. The solvent was removed under vacuum, and the yellow-orange powder obtained was crystallized from a CH_2Cl_2/*n*-hexane (1/1) bilayered mixture to yield orange crystals (1.08 g, 95%). IR (CH_2Cl_2): ν(CO)/cm^{-1} 2100, 2048. IR (CsI): ν(CO)/cm^{-1} 2088, 2034. ^{1}H NMR (CD_2Cl_2): δ 2.15 (s, CH_3). ^{13}C NMR (CD_2Cl_2): δ 156 (s, Ir−CO), −16.6 (q, CH_3, $^1J_{C-H}$ = 141 Hz). MS (FAB$^-$): *m*/*z* 646. Anal. Calcd for $C_{39}H_{33}IrI_3NO_2P_2$: C, 39.61; H, 2.81; N, 1.18. Found: C, 39.51; H, 2.72; N, 1.23.

6.5. $[Ir_2I_2(CH_3)_2(\mu\text{-}I)_2(CO)_4]$ (5′). This dimeric species can be prepared according to the procedure described by Ghaffar et al.[27] via abstraction of an iodide ligand from $[PPN][IrI_3(CH_3)(CO)_2]$. To 2 g (1.69 mmol) of the starting compound dissolved in 20 mL of dichloromethane was added InI_3 (0.83 g, 1.69 mmol). The mixture was stirred for 30 min at room temperature, and then the solvent was removed under vacuum to obtain a mixture of $[IrI_2(CH_3)(CO)_2]_2$ and $[PPN][InI_4]$. The dimer **5′** was repeatedly extracted from this powder using hot cyclohexane. The solvent was then removed under vacuum to obtain an orange-red powder (0.45 g, 25%). IR (CH_2Cl_2): ν(CO)/cm^{-1} 2120, 2074. ^{1}H NMR (CD_2Cl_2): δ 1.90, 1.85 (s, Ir−CH_3). ^{13}C NMR (CD_2Cl_2): δ 152.5, 150.4, 150.1 (s, Ir−CO), −5.3, −8.76, (q, CH_3, $^1J_{C-H}$ = 140 Hz).

6.6. $[IrI_2(CH_3)(CO)_3]$ (6). The dimer $[Ir_2I_2(CH_3)_2(\mu\text{-}I)_2(CO)_4]$ (**5′**; 1 g, 0.97 mmol) was dissolved in 20 mL of dichloromethane and placed in a glass reactor, which was then pressurized to 5 bar of CO and heated to 30 °C. The solution was stirred for 10 min and then cooled to −30 °C with an acetone/liquid nitrogen mixture. A 15 mL portion of *n*-heptane was added by the liquid feed line. After a few hours we observed the formation of microcrystals not suitable for X-ray analysis. IR (CH_2Cl_2): ν(CO)/cm^{-1} 2156, 2116, 2096. ^{1}H NMR (CD_2Cl_2): δ 2.08 (s, CH_3). ^{13}C NMR (CD_2Cl_2): δ 146.9 (s, Ir-CO), −22.3 (q, CH_3, $^1J_{C-H}$ = 140 Hz).

6.7. *mer,trans*-$[PPN][Ir(COCH_3)I_3(CO)_2]$ (8-PPN). This complex was prepared by addition of H_2O (2 g, 0.11 mol) to a solution of $[PPN][IrI_3(CH_3)(CO)_2]$ (0.5 g, 0.42 mmol) in 30 mL of methanol. The solution was placed in a glass reactor and stirred for 1 h under 5 bar of CO at room temperature. Then 20 mL of *n*-hexane was added by a liquid feed line overpressurized with CO and the reactor was cooled to 0 °C. After 2 h we observed the formation of orange crystals (0.38 g, 75% yield) suitable for X-ray analysis, corresponding to *mer,trans*-$[PPN][Ir(COCH_3)I_3(CO)_2]$. IR ($CH_2Cl_2$): ν(CO)/cm^{-1} 2114, 2070, 1655. ^{1}H NMR (CD_2Cl_2): δ 2.76 (s, CH_3). ^{13}C{^{1}H} NMR (CD_2Cl_2): δ 201.5 (COMe), 162.7 (s, Ir−CO), 52.2 (q, Me, $^1J_{C-H}$ = 140 Hz).

Crystallographic data for *mer,trans*-$[PPN][Ir(COCH_3)I_3(CO)_2]$ (8-PPN): $C_{40}H_{33}I_3IrNO_3P_2$, crystal dimensions 0.19 × 0.23 × 0.40 mm, monoclinic, space group $P2_1/c$, a = 14.605(1) Å, b = 18.580(1) Å, c = 15.176(1) Å, β = 95.168(6)°, V = 4101.4(5) Å^3, T = 180(2)K, Z = 4, D_c = 1.96 Mg/m^3, μ = 5.628 mm^{-1}. A total of 39 257 reflections was collected (R_{int} = 0.05), with θ_{max} = 32°. Semiempirical from equivalent absorption correction. Final *R* indices ($I > 2\sigma(I)$) were R1 = 0.0397 and wR2 = 0.0436.

6.8. *fac,cis*-$[PPN][Ir(COCH_3)I_3(CO)_2]$ (8-PPN). The salt $[PPN][IrI_3(CH_3)(CO)_2]$ (0.5 g, 0.42 mmol) was dissolved in 40 mL of dichloromethane containing 5 mL of methanol. The solution was placed in a glass reactor and stirred for 90 min under 5 bar of CO at room temperature. Then 20 mL of *n*-hexane was added by a liquid feed line and the reactor was cooled to 0 °C. After 2 h we observed the formation of yellow crystals (380 mg, 75% yield), corresponding to *fac,cis*-$[PPN][Ir(COCH_3)I_3(CO)_2]$. IR ($CH_2Cl_2$): ν(CO)/cm^{-1} 2111, 2061, 1679, 1660. ^{1}H NMR (CD_2Cl_2): δ 3.13 (s, CH_3). ^{13}C{^{1}H} NMR (CD_2Cl_2): δ 196.2 (COMe), 151.4 (s, Ir−CO), 49.5 (q, Me, $^1J_{C-H}$ = 140 Hz).

7. Synthesis of Platinum Complexes. 7.1. $[PtI_2(CO)_2]$ (10) and $[PtI_2(CO)]_2$ (10′). According to the literature,[28] $[PtI_2(CO)_2]$ was prepared by addition of PtI_2 (2 g, 4.45 mmol) to 125 mL of *n*-hexane in an autoclave. The mixture was pressurized with 12 bar of CO and stirred for 1 h at 75 °C. By using a high-pressure IR cell reactor, we observed the formation of the complex. The solution was cooled to room temperature in the reactor and then depressurized. A 1.69 g amount (80% yield) of a red solid was obtained and dried under reduced pressure, corresponding to the dimer $[PtI_2(CO)]_2$.

Under CO this compound reverts to $[PtI_2(CO)_2]$ in 100% yield. $[PtI_2(CO)]_2$ spectral data: IR (CH_2Cl_2) ν(CO)/cm^{-1} 2111; ^{13}C NMR (CD_2Cl_2) δ 154.5 (s + satellites (d), CO, $^1J_{Pt-C}$ 1843 Hz); ^{195}Pt NMR (CD_2Cl_2) δ −5328 ($^1J_{Pt-C}$ = 1843 Hz). $[PtI_2(CO)_2]$ spectral data: IR (CH_2Cl_2) ν(CO)/cm^{-1} 2127; ^{13}C NMR (CD_2Cl_2) δ 166.0 (s + satellites (d), CO, $^1J_{Pt-C}$ = 1466 Hz); ^{195}Pt NMR (CD_2Cl_2) δ −5790 ($^1J_{Pt-C}$ = 1466 Hz).

7.2. $[PPN][PtI_3(CO)]$ (9-PPN). $[PtI_2(CO)]_2$ (1 g, 1.05 mmol) was dissolved in 50 mL of dichloromethane, and HI (0.26 g, 2.10 mmol) was added to give rapidly, at room temperature, the complex $H[PtI_3(CO)]$.[28] Then, [PPN]Cl (1.20 g, 2.10 mmol) was added to the solution. The solvent was removed under vacuum to give a yellow product. Crystallization of this compound in a 1/1 CH_2Cl_2/*n*-hexane bilayered mixture gave yellow crystals of $[PPN][PtI_3(CO)]$ (1.08 g, 45%). IR (CH_2Cl_2): ν(CO)/cm^{-1} 2075. ^{13}C NMR (CD_2Cl_2): δ 152.8 (s + satellites (d), CO, $^1J_{Pt-C}$ = 1759 Hz). ^{195}Pt NMR (CD_2Cl_2): δ −5460 ($^1J_{Pt-C}$ = 1759 Hz). MS (FAB$^-$): *m*/*z* 603. Anal. Calcd for $C_{37}H_{30}I_3NOPtP_2$: C, 38.90; H, 2.65; N, 1.23. Found: C, 39.02; H, 2.61; N, 1.28.

Crystallographic data for 9-PPN: $C_{37}H_{30}I_3NOP_2Pt$, crystal dimensions 0.47 × 0.34 × 0.2 mm, monoclinic, space group $P2_1/c$, a = 13.6476(7) Å, b = 17.9405(9) Å, c = 15.4626(9) Å, β = 104.570(5)°, V = 3664.2(3) Å^3, T = 293(2) K, Z = 4, D_c = 2.071 Mg/m^3, μ = 6.474 mm^{-1}. A total of 22 953 reflections was collected (R_{int} = 0.0302), with θ_{max} = 26.32°. Semiempirical from equivalent absorption correction. Final *R* indices ($I > 2\sigma(I)$) were R1 = 0.0345 and wR2 = 0.0741.

8. Characterization of the Hetero- and Homobimetallic Complexes $[PPN][IrI_2(CH_3)(CO)_2(\mu\text{-}I)PtI_2(CO)]$ and $[PPN][Ir_2I_4(\mu\text{-}I)(CH_3)_2(CO)_4]$. We did not succeed in isolating these two compounds, but by correlating FAB/MS and NMR analyses we were able to characterize them in solution. $[PPN][IrI_3(Me)(CO)_2]$ (**4-PPN**; 0.12 g, 0.10 mmol) was dissolved in 50 mL of dichloromethane, and $[PtI_2(CO)]_2$ (0.03 g, 0.016 mmol) was added to the solution; IR analysis revealed that the reaction is almost instantaneous and gives a mixture of $[PPN][IrI_2(CH_3)(CO)_2(\mu\text{-}I)PtI_2(CO)]$ (**11-PPN**) and $[PPN][Ir_2I_4(\mu\text{-}I)(CH_3)_2(CO)_4]$ (**13-PPN**).

8.1. $[PPN][IrI_2(CH_3)(CO)_2(\mu\text{-}I)PtI_2(CO)]$ (11-PPN). IR (CH_2Cl_2): ν(CO)/cm^{-1} 2107, 2050. ^{1}H NMR (CD_2Cl_2): δ 2.36 (s, CH_3). ^{13}C NMR (CD_2Cl_2): δ 155.4 (s, CO), 154.91 (s + satellites (d), Pt−CO, $^1J_{Pt-C}$ = 1650 Hz), −14.09 (q, CH_3, $^1J_{C-H}$ = 141 Hz), −14.18 (q, CH_3, $^1J_{C-H}$ = 141 Hz). ^{195}Pt NMR (CD_2Cl_2): δ −5462 ($^1J_{Pt-C}$ = 1650 Hz). MS (FAB$^-$): *m*/*z* 1121.

8.2. $[PPN][Ir_2I_4(\mu\text{-}I)(CH_3)_2(CO)_4]$ (13-PPN). IR (CH_2Cl_2): ν(CO)/cm^{-1} 2117, 2061. ^{1}H NMR (CD_2Cl_2): δ 2.28 (s, CH_3). ^{13}C NMR (CD_2Cl_2): δ 154.68 (s, CO), −14.83 (q, CH_3, $^1J_{C-H}$ = 141 Hz). MS (FAB$^-$): *m*/*z* 1161.

Acknowledgment. This work was supported by Acetex Chimie and by the "Ministère de la Recherche et de la Technologie". G.L. thanks the Swiss National Science Foundation (Grant 200020-105335/1).

Supporting Information Available: CIF files giving X-ray crystallographic data for ***mer,trans*-8-PPN** and **9-PPN**. This material is available free of charge via the Internet at http://pubs.acs.org.

OM060282X

(27) Ghaffar, T.; Adams, H.; Maitlis, P. M.; Sunley, G. J.; Baker, M. J.; Haynes, A. *Chem. Commun*. **1998**, 1023.

(28) Andreini, B. P.; Dell'Amico, D. B.; Calderazzo, F.; Venturi, M. G. *J. Organomet. Chem*. **1988**, 357.